

# ReCoM: Realistic Co-Speech Motion Generation with Recurrent Embedded Transformer

Yong Xie<sup>1</sup> Yunlian Sun<sup>1</sup> Hongwen Zhang<sup>2</sup> Yebin Liu<sup>3</sup> Jinhui Tang<sup>1</sup>

<sup>1</sup>Nanjing University of Science and Technology <sup>2</sup>Beijing Normal University <sup>3</sup>Tsinghua University

## Abstract

We present *ReCoM*, an efficient framework for generating high-fidelity and generalizable human body motions synchronized with speech. The core innovation lies in the Recurrent Embedded Transformer (RET), which integrates Dynamic Embedding Regularization (DER) into a Vision Transformer (ViT) core architecture to explicitly model co-speech motion dynamics. This architecture enables joint spatial-temporal dependency modeling, thereby enhancing gesture naturalness and fidelity through coherent motion synthesis. To enhance model robustness, we incorporate the proposed DER strategy, which equips the model with dual capabilities of noise resistance and cross-domain generalization, thereby improving the naturalness and fluency of zero-shot motion generation for unseen speech inputs. To mitigate inherent limitations of autoregressive inference, including error accumulation and limited self-correction, we propose an iterative reconstruction inference (IRI) strategy. IRI refines motion sequences via cyclic pose reconstruction, driven by two key components: (1) classifier-free guidance improves distribution alignment between generated and real gestures without auxiliary supervision, and (2) a temporal smoothing process eliminates abrupt inter-frame transitions while ensuring kinematic continuity. Extensive experiments on benchmark datasets validate *ReCoM*'s effectiveness, achieving state-of-the-art performance across metrics. Notably, it reduces the Fréchet Gesture Distance (FGD) from 18.70 to 2.48, demonstrating an 86.7% improvement in motion realism. Our project page is <https://yong-xie-xy.github.io/ReCoM/>.

## 1. Introduction

Human motion generation is a broad concept aimed at creating natural, realistic, and diverse human motions, including whole-body movements such as walking, jumping, dancing, etc. Recently, many excellent works have emerged, such as [3, 13, 27, 35, 40, 50], all of which have made outstanding contributions to the field of human motion generation.

Co-speech gesture generation is an important subtask in the field of human motion generation. It involves the automatic generation of expressions and gestures that are seamlessly aligned with speech. And it primarily focuses on upper-body movements, including the motion of the body, hands, and face. This research area holds significant importance for human-computer interaction, digital entertainment, virtual reality, intelligent robots, and other domains. These gestures can help to enrich speech presentation, thus achieving a more natural and fascinating communication experience.

Currently, co-speech gesture generation technology primarily relies on deep learning models. Popular models include Generative Adversarial Networks (GANs) [12], Variational Autoencoders (VAEs) [18], Vector Quantized Variational Autoencoders (VQ-VAE) [42], and Diffusion Models [17, 34, 36]. These models are capable of understanding the intricate interactions between speech signals and gestures, enabling them to generate gestures that are consistent with the speech content.

Presently, the field of gesture generation has drawn significant attention. Studies such as those in [29, 46] use VQ-VAE. [51] uses the residual VQ-VAE [24]. Studies in [28, 29] manage to perform the step-by-step processing and transformation of data by means of cascaded architectures. The study in [33] takes DiT [32] as its main architecture. Furthermore, studies [4, 6, 7, 53] adopt diffusion models as their principal architectures. Moreover, the research in [31] introduces product quantization to the VAE and enriches the representation of complex holistic motion.

Though achieving impressive results, these approaches face some challenges. One challenge is how to ensure that the model learns appropriate gesture features that meet the demand of fidelity and generalization. Another challenge is that large gesture datasets are difficult to acquire. Fortunately, many good pose estimation methods were proposed [41, 45, 48, 49], fulfilling the need for acquiring high-quality datasets. Hence, we put our emphasis on addressing the first challenge.

Our motivation for *ReCoM* mainly stems from two observations. Firstly, we noticed that previous methods don't

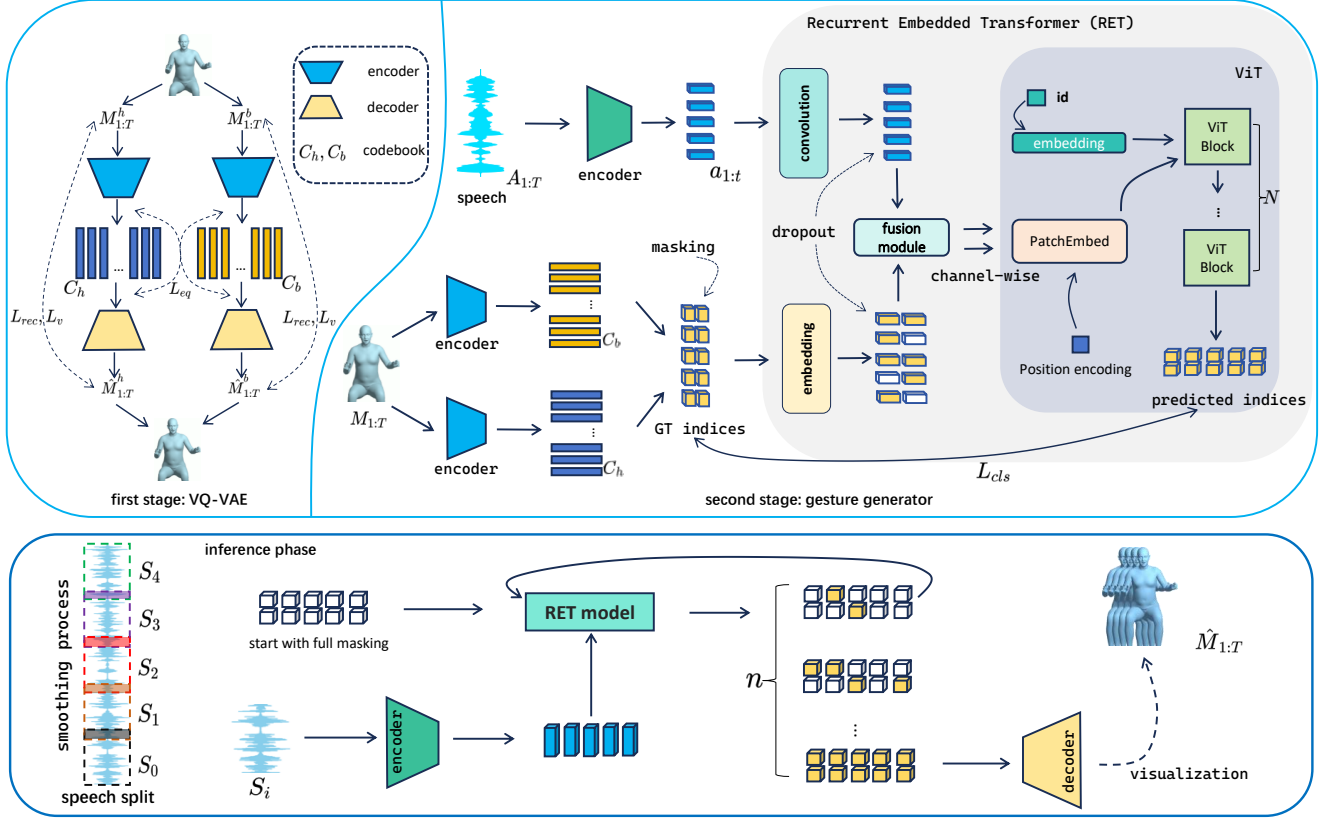


Figure 1. The gesture training and inference pipeline of our work. Given an audio input, our method aims to produce a high-fidelity gesture. We use the loss function  $L_{VQ}$  to optimize the compositional VQ-VAEs, enabling them to learn discrete gesture representation. We carefully employ effective data processing strategies to optimize the gesture generator, enabling it to obtain high-fidelity results. In the Inference phase,  $S_i$  denotes the  $i$ -th speech segment. In this phase, we use IRI and a temporal smoothing process. The RET model is our gesture generator. Additionally,  $n$  denotes the number of iterations, which is a variable value depending on the input. The novel inference strategy further enhances the model’s performance in a non-autoregressive way. Most of the variables mentioned in the paper are introduced in Sec. 3, while the remaining variables are mentioned in Sec. 4.1, Sec. 4.2, and Sec. 4.3.

adequately fit the dataset, meaning these models might lack sufficient learning ability. For instance, we observed that the Habibi *et al.* method [14] generates gestures with excessively large jitter amplitudes. TalkSHOW [46], which occasionally produces jittery motions, frozen movements, and noticeable penetration in animation, results in low fidelity. Secondly, we observed that previous studies don’t pay sufficient attention to generalization, meaning that their performance on out-of-domain datasets is poor. For instance, ProbTalk [31] demonstrates suboptimal performance on generalization datasets, and sometimes its visualized motions are overly slow. Given humans’ strong perceptual sensitivity to unnatural human motions, this series of problems may lead to a poor user experience when applied.

In addition, the works mentioned above rarely focus on both temporal and spatial information simultaneously. Due to the aforementioned issues, we propose some cor-

responding improvement strategies. Our method is based on [46], and our solution draws inspiration from [20], and [13]. Since handling spatial information presents more challenges, we focus on this issue in this work. Specifically, we leverage ViT to design our core architecture: Recurrent Embedded Transformer (RET). RET incorporates channel-wise operations that optimize it for spatial information processing. Other architecture choices include adopting VQ-VAE to learn two discrete gesture representations respectively for body and hand, and using an encoder-decoder architecture for face generation.

Our model’s competitive results is evident from the comparisons detailed in Sec. 6.1. We believe that the effectiveness of our method mainly stems from **three improvements**. The first improvement involves an innovatively-designed RET based on the ViT architecture. The RET module enhances the fidelity of generated gestures through iterative refinement during inference. It employs channel-

wise operations where hand and body features are processed separately in distinct channels, analogous to image processing frameworks. This disentanglement of body parts enables precise anatomical differentiation while endowing RET with more comprehensive spatial information processing capabilities. For detailed information, please refer to Sec. 4.3.

The second improvement is the implementation of the key data processing strategy. It is Dynamic Embedding Regularization (DER). This method applies dropout[11, 37] operations after the embedding layer. The dropout mechanism remains active during training but is disabled during inference. This is crucial for enhancing the model’s learning ability, as it reduces the complex co-adaptations [37] in large models and meanwhile introduces more noise to enhance the model’s robustness. Moreover, thanks to the characteristic of this strategy that helps in reducing overfitting, it effectively improves the generalization ability of the model. In addition, in order to adapt to the IRI strategy and enhance the model’s robustness, we applied the “masking” operation to the ground truth (GT). Specifically, we randomly mask some GT data and then train the RET model to predict the clean GT, as shown in Fig. 1.

To further overcome the disadvantages of autoregressive inference like error accumulation and the lack of self-correcting mechanisms, we propose the third improvement to optimize the inference phase. During inference, we apply Iterative Reconstruction Inference (IRI) to ensure the effectiveness of the masking strategy. Unlike the training phase, the IRI strategy starts with completely masked indices (indices are the positions within a codebook). It predicts indices with high confidence, and iteratively uncovers the remaining masked indices. For a more detailed discussion on the IRI strategy, please refer to Sec. 5. To further enhance the model performance and the visual perception effect of the generated results, we introduce Classifier-Free Guidance (CFG) [16] and the temporal smoothing process. For more details, please refer to Sec. 4.4 and Sec. 5.2.

After implementing the aforementioned strategies, our model outperforms those of previous work from the experimental results in Sec. 6.1. Our results demonstrate that our method exhibits better and more stable generation performance when applied in practice.

In summary, our contributions are as follows:

- Our work leverages the structural characteristics of ViT to design the RET. By incorporating channel-wise operations, the model effectively perceives and processes spatio-temporal information. Additionally, we preserve the inherent advantages of the ViT model, specifically its scalability and compatibility with other models. Our work provides certain theoretical support for the selection of model structures in the field of gesture generation.
- By deploying the DER strategy, we significantly enhance

the model’s learning capability. Moreover, thanks to the DER strategy’s characteristic of reducing overfitting, the DER strategy effectively improves the generalization ability of the model. Thereby, the model avoids the generation of frozen movements or penetration in animation when handling out-of-domain audio inputs.

- Previous methods usually use autoregressive inference. Since it relies too heavily on previously generated data, such heavy reliance often leads to error accumulation and a lack of self-correcting mechanisms. To address these limitations, we propose a novel inference strategy (IRI), adopt the CFG strategy with prudence, and explore a temporal smoothing process suitable for Transformer-encoder models. These strategies have a positive impact on the model.

## 2. Related Work

In early co-speech gesture generation research, rule-based systems were commonly used. These methods defined manually-made rules to synchronize speech and gestures. Specific speech elements triggered corresponding gestures, like a pointing gesture for object-related nouns or a waving one for greetings, making gestures highly semantic. However, they had limitations. They demanded much manpower for rule design and maintenance, and lacked flexibility, struggling to adapt to diverse speaking styles and contexts. Relevant literature comprehensively reviews these methods [19, 21, 44].

To alleviate the problems existed in the rule-based methods mentioned above, a large number of data-driven methods are proposed. [15] uses a bidirectional Long Short-Term Memory to generate gestures from audio utterances. By learning the audio-gesture relationships, it predicts the full-skeleton human postures at each time step and then performs temporal filtering to smooth the posture sequences. [22] extends the work of [15]. It removes the need for temporal smoothing through representation learning of autoencoders and converts audio input into gesture sequences in the form of 3D joint coordinates. [9, 10] adds multiple adversarial objectives to recurrent neural networks to deal with the problem of regression to the mean that is likely to occur in long sequences. They also consider the phase structure of gestures, motion realism, displacement and the diversity of mini-batches. [1] learns to implicitly estimate the mixture density to achieve the transfer of different speaker styles. Through adversarial training, the generated gestures can represent the styles of different speakers. [2] extends the normalization-flow-based model to speech-driven gesture synthesis, achieving style control. The generated gestures perform well in terms of naturalness and appropriateness. [14] presents a speech-driven 3D gesture synthesis approach. It has a generator and discriminator. The generator converts audio features to 3D pose sequences. Trained

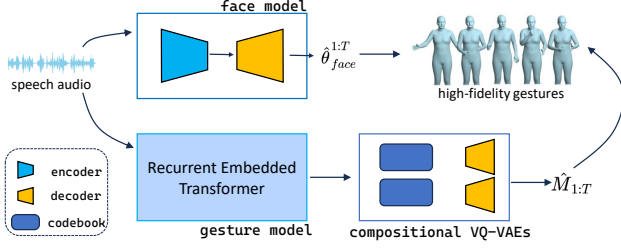


Figure 2. Our ReCoM pipeline consists of three components: a face generator, a gesture generator and a compositional VQ-VAE. By inputting speech audio, we can obtain the corresponding gesture sequence. Among them, the face model is responsible for generating the facial movement sequence  $\hat{\theta}_{face}^{1:T}$ . The gesture generator aims to generate gesture indices with high confidence. These indices are then input to the compositional VQ-VAE for nearest neighbor search and decoding to obtain the gesture sequence  $\hat{M}_{1:T}$ .

with regression and adversarial losses, it generates gestures in sync with speech. [25] uses conditional VAE to convert speech into diverse gestures. It models the speech-gesture mapping by splitting the cross-modal latent code into shared code and motion-specific code. [39] adopts the conditional Flow-VAE framework to generate the spontaneous gestures of the speaker and listener roles in conversations. It trains the model through an autoregressive framework and improves the expressiveness of the generated gestures. [52] generates gesture videos that match unseen audio inputs by conducting audio-video searches in the video gesture database. It uses video motion graphs and the beam search algorithm to find the optimal order of gesture frames.

Recently, [4] uses multi-modal inputs and latent diffusion models. It learns motion via VQ-VAE and synthesizes gestures in the latent space. With contrastive learning and AdaIN layer, it realizes flexible style-controlled co-speech gesture synthesis. [29] presents EMAGE to generate full-body gestures from audio and masked gestures. It creates BEAT2 and applies specific techniques for joint optimization, promoting the field.

### 3. Pipeline Overview

Given a speech recording, the goal of our ReCoM is to generate high-fidelity gestures corresponding to it. The overall pipeline is depicted in Fig. 2. In our method, we use  $\theta_{face} \in \mathbb{R}^{103}$  to represent the whole face parameter. It consists of  $\theta_j$  and  $\theta_e$ , where  $\theta_j \in \mathbb{R}^3$  represents jaw pose and  $\theta_e \in \mathbb{R}^{100}$  represents FLAME [26] expression parameters.  $M_{1:T}$  denotes a  $T$  frame gesture clip, and  $\hat{M}_{1:T}$  represents the corresponding reconstructed gesture clip.  $T$  is the number of the fixed frames used during training.  $M^b$  and  $M^h$  represent body pose and hand pose.  $E_{1:t} = \{e_1, \dots, e_t\} \in \mathbb{R}^{t \times 64}$  denotes codebook vectors, and  $Z_{1:t} = \{z_1, \dots, z_t\} \in \mathbb{R}^{t \times 64}$

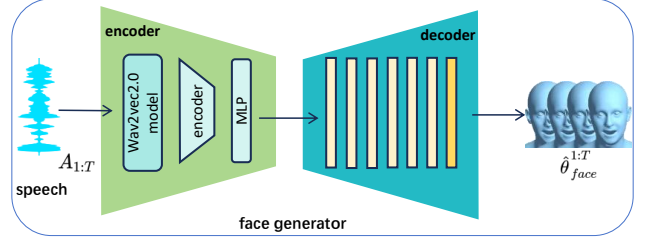


Figure 3. For face generator, we choose encoder-decoder architecture.

denotes latent vectors, and  $t = \frac{T}{4} = 22$ .  $A_{1:T}$  is the MFCC feature of audio. And  $id$  represents the speaker’s identity drawn from a predefined identity set.

## 4. Method

### 4.1. Face Generator

For the face, following [46], we adopt an encoder-decoder architecture, as illustrated in Fig. 3. Owing to the excellent capability of learning audio representation, we adopt wav2vec 2.0 [5] as the backbone. The decoder consists of multiple temporal convolution layers. We construct the face parameter distribution through loss function as follows:

$$L_{face} = L_{jaw}(\theta_j, \hat{\theta}_j) + L_{expression}(\theta_e, \hat{\theta}_e), \quad (1)$$

where  $L_{jaw}$  and  $L_{expression}$  are the L1 and L2 reconstruction losses.  $\hat{\theta}$  denotes the corresponding reconstructed feature.

### 4.2. Gesture Codebook

In the process of reconstructing and generating the hand and upper body parts, we use a **two-stage** approach. In the **first stage** we use VQ-VAE [42], which can learn a discrete representation and ensure that the poses are accurately reconstructed through latent vectors.

Our goal in this stage is to train VQ-VAE well enough to reconstruct pose data, preparing it for the generation task in the next stage. We use a loss function  $L_{VQ}$  that includes reconstruction loss  $L_{rec}$ , codebook loss  $L_{eq}$ , and reconstruction speed loss  $L_v$  as follows:

$$L_{VQ} = L_{rec}(M_{1:T}, \hat{M}_{1:T}) + L_{eq}(Z_{1:t}, E_{1:t}) + L_v(M_{1:T}, \hat{M}_{1:T}), \quad (2)$$

$$L_{eq} = \|sg[E_{1:t}] - Z_{1:t}\| + 0.25\|E_{1:t} - sg[Z_{1:t}]\|, \quad (3)$$

$$L_v = \frac{1}{T-1} \sum_{i=1}^{T-1} |(M_{1:T-1} - M_{2:T}) - (\hat{M}_{1:T-1} - \hat{M}_{2:T})|, \quad (4)$$

where **sg** denotes stop gradient operation.  $L_{rec}$  is Mean Absolute Error loss. We learn two VQ-VAE for the hand



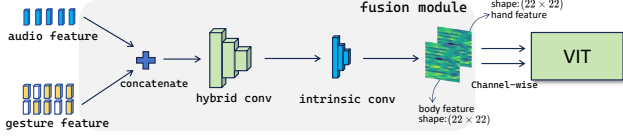


Figure 4. Fusion module. We apply hybrid convolution (with a downsampling rate of 2 and a convolution kernel of  $1 \times 1$ ) to fuse audio features and gesture features. The role of hybrid convolution here is to combine the audio and gesture features, enabling them to interact and form a unified feature representation. Then, we use intrinsic convolution to obtain the essential mixed features. Intrinsic convolution serves to downsample the mixed features into the latent space. This downsampling operation is crucial as it allows the ViT module to process the data without the need for an overly large number of parameters. Finally, we input the features into the ViT model by adopting a channel-wise strategy.

and upper body, with their codebooks respectively designated as  $C_h$  and  $C_b$ . The  $C_h$  quantizes  $M^h \in \mathbb{R}^{T \times 90}$ , and the  $C_b$  quantizes  $M^b \in \mathbb{R}^{T \times 63}$ . In training phase, we first encode the inputs  $M_{1:T}$  into an embedding  $Z_{1:t}$ , then we use a Nearest Neighbor Search to return codebook indices. Lastly, we retrieve the corresponding embedding  $E_{1:t}$  for input to the decoder to reconstruct the poses  $\hat{M}_{1:T}$ . We train the model using the loss function  $L_{VQ}$ .

### 4.3. Gesture Generator

The **second stage** focuses on generating high-fidelity gestures and enhancing the generalization of the model. The gesture generator’s core is the ViT [20]. To save training time, we train the generator in the indice space of the codebook, with the loss function employing only **cross-entropy loss** as follows:

$$L_{cls} = CrossEntropy(I_{1:t}, ViT(fusion(I_{1:t}, a_{1:t}, id))), \quad (5)$$

where  $I \in \mathbb{R}^{t \times 2}$  denotes the indices of poses. *fusion* module is shown in Fig. 4.  $a_{1:t}$  represents the audio feature after downsampling.  $I_{1:t}^m$  denotes the indices of poses being masked.

Due to the challenge of establishing a mapping from audio to gestures, depending solely on audio input complicates the convergence of training. Therefore, to accelerate loss convergence, we incorporate the GT pose as an additional input for auxiliary. Thus, our gesture generator is fed with  $A_{1:T}$  and GT pose  $M_{1:T}$  data in the training phase.

As shown in Fig. 1, we first use two codebook encoders to get pose indices  $I_{1:t}$  and use an audio encoder and  $1 \times 1$  convolution to get audio feature  $a_{1:t}$ . Then, we apply a masking strategy (like [8]) to  $I_{1:t}$  and pass the masked  $I_{1:t}$  through an embedding layer to map  $I_{1:t}$  and  $a_{1:t}$  to the same dimensions. For pose features, we employ a dropout strat-

egy to enhance the model’s learning capability by introducing random perturbations. Later, we fuse the audio and pose features using a fusion module and then input them into the ViT model. Notably, the input operation is carried out channel-wise, splitting the body and hand poses into two channels (injecting spatial information into the third dimension of the features). This is similar to an RGB image (shape is width  $\times$  height  $\times$  2), where each channel represents different components yet is closely interconnected. As shown in Fig. 4, we divide the hand features and body features into two feature maps. Meanwhile, the width and height of the feature maps correspond to the temporal and spatial dimensions of the gesture clips respectively. For the spatial dimension corresponding to the width, we do not perform compression, while for the feature dimension corresponding to the height, we conduct downsampling using intrinsic convolution. Thus, channel-wise processing is crucial for the effectiveness of the RET model, as it is essential to fuse spatio-temporal information.

In the ViT model, we first apply patchEmbed to different channels of the input data. Then, we add *id* and position encoding, both of which are fed into  $N$  ViT blocks ( $N$  is 15) to obtain the predicted indices  $\hat{I}$ . Finally, by applying the loss function to  $I$  and  $\hat{I}$ , we can train the model to converge.

### 4.4. Training Detail

In our experiments, we find that if we only input speech data, the model is hard to converge. Thus, we combine speech and GT pose as input data. But, if the GT pose isn’t processed, the model is prone to overfitting. After extensive experimentation, we find that DER and masking strategies can help to alleviate overfitting. These strategies introduce large random perturbations to the input data, not only guiding the model to learn more robust features, but also improving the generalization ability of the model. Additionally, we employ channel-wise operation to fuse spatio-temporal information, and apply an Exponential Moving Average (EMA) technique during model training.

We use CFG [16] to train our model. Firstly, we try to disable the speech  $a_{1:t}$  (i.e. Empty condition) in Eq. (5) with a probability of 10% like [16], but it fails to work as expected. Thus, we directly employ the dropout operation to substitute the Empty condition, which effectively enhances the performance of the model. During inference, we use the following Eq. (6) in the last neural network layer before softmax to guide the generation process:

$$logit = s \cdot RET(a_{1:t}, id) - (s - 1) \cdot RET(\phi, id), \quad (6)$$

where  $s$  is guidance scale, and *logit* is the guided generation result. We can control the speaker gesture style through *id*. It is worth noting that, in order to achieve good results, the linear combination in Eq. (6) we adopted is different

Table 1. **A** represents training with the Empty condition at a certain probability. **B** denotes training with the dropout operation at a certain probability. **C** represents using neither of the two ways, i.e., not conducting any processing on the speech condition. **EN** represents enabling Eq. (6) during inference, while **UN** represents not enabling.

Method	Diversity $\uparrow$	FGD $\downarrow$	MAE $\downarrow$	BC $\rightarrow$
A and UN	8.4988	30.1020	35.5114	0.8570
A and EN	9.3009	100.1004	35.8544	0.8569
B and UN	8.2614	10.8462	<b>35.4285</b>	0.8574
B and EN	8.9830	<b>2.4816</b>	35.9665	<b>0.8579</b>
C and UN	8.3830	16.7449	35.4646	0.8567
C and EN	<b>10.9710</b>	143.0840	36.6753	0.8578

from that in [16]. In addition, we conduct experiments, as shown in Tab. 1, to prove that in our model, it is better to use dropout than the Empty condition during training. As the results show, among these three methods (A, B, and C), when the CFG inference is utilized, employing the Empty condition or not processing the speech condition has a negative effect on the model performance. Using the dropout operation in combination with the CFG inference instead has a positive effect.

## 5. Inference Phase

In the inference phase, we divide the process into two parts: face inference and gesture inference. For face inference, we have the VAE architecture as mentioned in Sec. 4.1. Given an audio input, the facial model trained on facial distributions can generate a FLAME [26] result.

### 5.1. Iterative Reconstruction Inference

For the gesture inference part, we propose a novel inference strategy, termed IRI, to enhance the generation results, as illustrated in Fig. 1. Specifically, the method initially takes speech features and fully masked motion indices as inputs. Then, we repeatedly input the indices and speech features into the RET model to predict masked indices until all the indices are recovered. In this process, the model automatically selects results that exceed the confidence threshold value. Indices with results below the threshold will be predicted in next iterations. The threshold value decreasing adaptively in a linear manner aims at reducing the difficulty of data reconstruction. This adjustment is necessary because some of the data, due to the accumulation of global errors, cannot achieve results with high confidence. Making predictions completely out of chronological order helps alleviate the cumulative errors in the time sequence. Moreover, by re-inputting the low-confidence indices into the RET model for prediction, the model can correct the low-

confidence results it generates.

### 5.2. Temporal Smoothing Process

Transformer encoder models [43] require the length of sequences to be strictly equal to the fixed length during training. To generate long gesture sequences, we need to concatenate different result segments. Initially, we use a direct concatenation strategy. However, this results in incoherence at the junctions of the generated outputs, similar to [31]. To address this issue, we need to suppress the excessive freedom of the RET model, guide the generation direction, and produce results that align more closely with human visual perception. With these goals in mind, we propose the Smoothing strategy as shown in Fig. 1. Surprisingly, this temporal smoothing process significantly improves the visual coherence of the overall results, not just at the connection points of the results. Specifically, we divide the speech audio into several short segments in chronological order. For an audio with frame rate of 30FPS, we split it into segments with 88 frames each. For the segments  $S_i$  other than the first one, we incorporate the last 8 frames of segment  $S_{i-1}$  into the segment  $S_i$ . This enables the information of several independent segments to be transmitted in a temporal sequence.

### 5.3. Editing Capabilities

Since we adopt the Transformer-encoder as the main architecture of the gesture generator, our RET model acquires certain editing capabilities. This means that by adding a target pose, it can generate gestures that match the target gesture. In addition, our model can smoothly splice two gesture clips together. Moreover, similar to the approach in [38] which uses residual VQ-VAE [24], we are able to independently control body or hand poses based on the characteristics of the VQ-VAE [42]. Please refer to supplementary material for editing examples.

## 6. Experiment

### 6.1. Quantitative Comparisons

We compare ReCoM with [14], TalkSHOW [46] and ProbTalk [31]. We select a series of metrics to ensure a comprehensive and accurate assessment of the model’s performance across multiple aspects.

**Diversity.** The metric follows [29] and represents the average L1 distance between  $K$  gesture clips. Its calculation formula is shown in Eq. (7):

$$L_1^{div} = \frac{1}{2K(K-1)} \sum_{t=1}^K \sum_i \|p_t^i - \bar{p}_t\|_1, \quad (7)$$

where  $p_t^i$  denotes the position of joints in frame  $i$  of the  $t$ -th gesture clip. Where  $\bar{p}_t$  represents the average value of the joint positions of the  $t$ -th gesture clip.

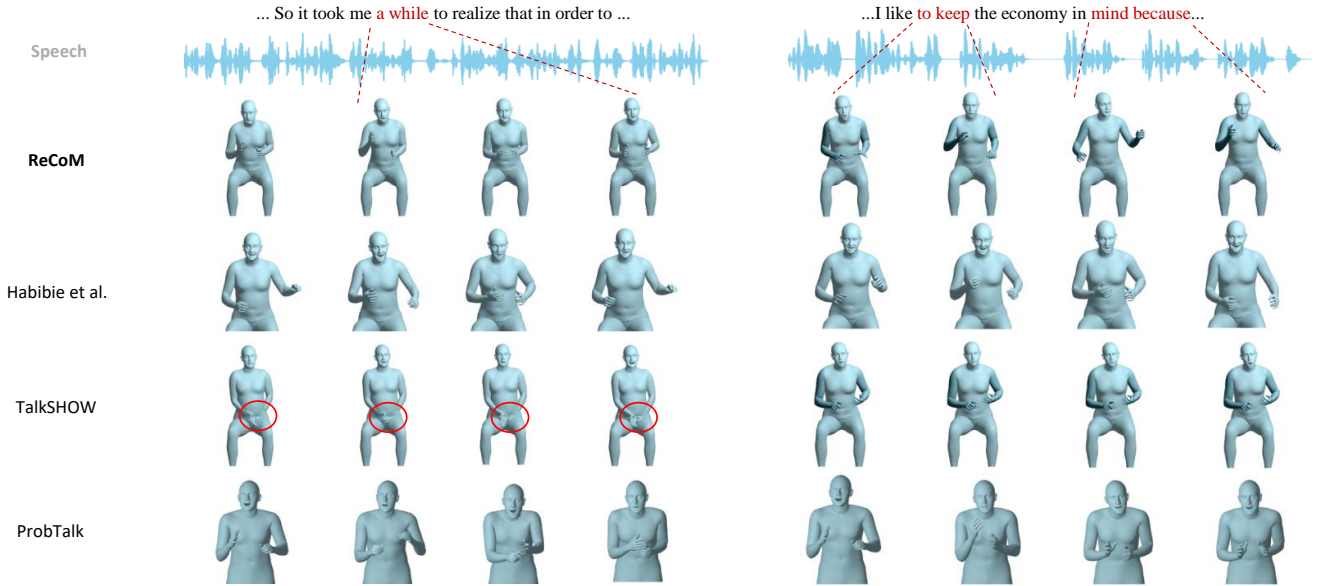


Figure 5. When receiving out-of-domain audio inputs, TalkSHOW exhibits a frozen motion for a number of seconds. The results of ProbTalk often show incoherence between two consecutive frames. Meanwhile, Habibie et al.’s method often generates gestures with overly large jitter amplitudes. Our ReCoM results instead remain natural. Please refer to supplementary materials for more video demos, with both in-domain and out-domain evaluation.

Table 2. In-domain evaluation on the **SHOW** dataset. The downward arrow indicates that smaller values are better, and vice versa for the upward arrow. The right-pointing arrow indicates that the closer the value is to the ground truth, the better. Bold and underlined indicate the best and the 2nd best results. And GT denotes Ground Truth.

Method	Diversity $\uparrow$	FGD $\downarrow$	MAE $\downarrow$	BC $\rightarrow$
GT	9.4850	0	0	0.8676
Habibie et al.	7.5246	239.1780	98.6942	0.9477
TalkSHOW	6.8678	66.1574	36.7540	<b>0.8713</b>
ProbTalk	<u>7.6758</u>	<u>18.7028</u>	<u>36.0005</u>	0.7837
ReCoM	<b>8.9830</b>	<b>2.4816</b>	<b>35.9665</b>	<u>0.8579</u>

Table 3. Out-of-domain evaluation on **BEAT2** without any fine-tuning.

Method	Diversity $\uparrow$	FGD $\downarrow$	MAE $\downarrow$	BC $\rightarrow$
GT	14.8500	0	0	0.8351
Habibie et al.	7.5242	239.1844	92.2333	0.9477
TalkSHOW	<u>8.6990</u>	<u>98.3199</u>	<u>72.2534</u>	0.8729
ProbTalk	8.2616	100.0674	<u>71.6509</u>	<u>0.8178</u>
ReCoM	<b>11.1303</b>	<b>96.7793</b>	<b>71.5830</b>	<b>0.8469</b>

**FGD (Frechet Gesture Distance).** Similar to the FID metric, it is an important metric for measuring the similarity between two multi-dimensional Gaussian distributions,

particularly suitable for assessing the performance of generative models at the feature space [23, 47]. A smaller FGD value indicates that the distribution of generated samples is closely aligned with the distribution of real samples, suggesting high fidelity of the model’s outputs.

**MAE (Mean Absolute Error).** It calculates the average of the sum of absolute differences between real and generated samples in the feature space.

**BC (Beat Consistency Score).** The objective of the BC metric is to gauge the correlation between the variation degree of human joint points and audio beats [30].

Experimental results, as reported in Tab. 2 and Tab. 3, demonstrate our model’s high fidelity and good generalization. The higher diversity metrics are attributed to non-autoregressive inference. That is, the model doesn’t rely on previously generated data, which improves the diversity. In addition, lower FGD and MAE metrics indicate that our model better fits the training dataset. The lower Beat Consistency (BC) metric might be attributed to the semantic association ability of our model. For instance, it can link the sound of clapping with the actual clapping motion, associate the word ”no” with the action of quickly opening the arms, and connect ”hip hop” to similar dance styles. Precisely because of this semantic association ability, the model tends to focus less on its own beat consistency, which in turn results in a lower BC metric.

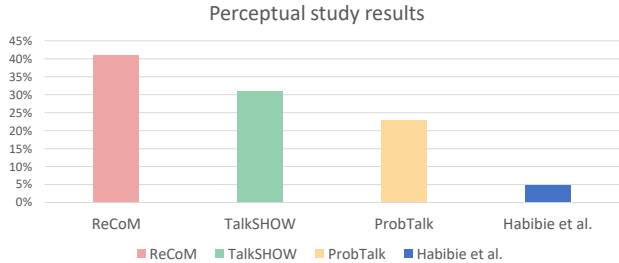


Figure 6. Perceptual study results. We calculate the win rate of the evaluation. Our method demonstrate higher overall preference of participants.

## 6.2. Qualitative Comparisons

As shown in Fig. 5, we present two gesture clips generated from an out-of-domain audio segment, displaying frame captures that span approximately four seconds. It can be observed that our method is capable of performing inference as usual when receiving out-of-domain audio inputs. However, due to the autoregressive method used in TalkSHOW [46], this results in error accumulation and a lack of self-correcting mechanisms, making it prone to producing frozen motion and occasional penetration in animation. Additionally, TalkSHOW often outputs the unnatural motions, e.g., keeping avatar’s left hand to one side. Due to our model’s non-autoregressive architecture, we don’t have these problems.

**Perceptual Study.** Objective metrics do not always reflect the model’s performance. Therefore, to further verify the visual performance of our ReCoM method, we conducted a perceptual study. In total, we sampled 81 videos. Among them, 50 were from the SHOW test set, while the remaining 31, including 5 long ones with a length of 60 seconds, were from the wild TED audio. Twenty participants evaluated videos generated by different methods presented in random order, selecting their most preferred option. The results are shown in the Fig. 6, and our method demonstrates higher overall preference among participants. Notably, although ProbTalk has better objective metrics than TalkSHOW, it achieved somewhat worse results in the perceptual study. We attribute this to the fact that the motions generated by ProbTalk are not smooth, often resulting in the phenomenon of “frame-skipping”, where there is a lack of coherence between consecutive frames in the video. We believe this may have a significant impact on the visual experience of the subjects.

## 6.3. Ablation Study

As shown in Tab. 4, to validate the effectiveness of our design, we conduct ablation experiments by removing these strategies. It can be observed that these strategies all have a significant impact on the FGD metric. Although the RET

Table 4. Our ablation results, which is tested on the SHOW dataset. **w/o** denotes “without”. **DER** means “Dynamic Embedding Regularization”.

	<i>Diversity</i> ↑	<i>FGD</i> ↓	<i>MAE</i> ↓	<i>BC</i> →
ReCoM	<b>8.9830</b>	<b>2.4816</b>	35.9665	<b>0.8579</b>
w/o CFG	8.2614	10.8462	35.4285	0.8574
w/o IRI	8.7314	39.9367	<b>31.7857</b>	0.8570
w/o audio-dropout	8.3830	16.7449	35.4646	0.8567
w/o EMA	8.1029	27.6172	35.4365	0.8570
w/o DER	6.9025	146.3948	35.2953	0.8545
w/o masking	8.4321	71.0111	35.6858	0.8560

model isn’t the best in all metrics, we choose it because FGD has the biggest impact on visual effect.

## 7. Conclusion, Limitation and Future Work

We design the RET by retaining the structural characteristics of ViT, and enable the model to process spatio-temporal information through channel-wise operations. Additionally, we apply some strategies to improve the model’s convergence procedure, and we use new inference strategy to enhance the generation results. This method achieves significant results, not only enhancing the model’s performance but also improving its generalization ability. Finally, our model’s design enables it to have certain editing capabilities.

It must be acknowledged that our model has a deficiency in terms of beat consistency, but we believe this trade-off is worthwhile. Furthermore, our work does not take into account lower body motion, resulting in a lack of overall body information. This can cause occasional penetration between the hand and lower body in seated poses, reducing the animation’s practicality. However, model penetration will hardly occur in the upper body and hands. Lastly, due to the self-correcting mechanism in our model, it occasionally generates faster movements as it attempts to correct errors made earlier.

In future work, we may try to combine multi-modal information, such as text, to enhance the semantic results of our model. Additionally, we hope to design a model capable of generating whole body gestures of high fidelity, including the lower body, which will be challenging yet highly practical. Meanwhile, we observe that the existing metrics can hardly fully test the performance of the model from a human perspective. Thus, we will attempt to propose more comprehensive evaluation metrics.

## References

[1] Chaitanya Ahuja, Dong Won Lee, Yukiko I. Nakano, and Louis-Philippe Morency. Style transfer for co-speech gesture animation: A multi-speaker conditional-mixture approach. In *European Conference on Computer Vision*, 2020. 3



- [2] Simon Alexanderson, Gustav Eje Henter, Taras Kucherenko, and Jonas Beskow. Style-controllable speech-driven gesture synthesis using normalising flows. *Computer Graphics Forum*, 39, 2020. 3
- [3] Simon Alexanderson, Rajmund Nagy, Jonas Beskow, and Gustav Eje Henter. Listen, denoise, action! audio-driven motion synthesis with diffusion models. *ACM Trans. Graph.*, 42(4), 2023. 1
- [4] Tenglong Ao, Zeyi Zhang, and Libin Liu. Gesturediffuclip: Gesture diffusion model with clip latents. *ACM Transactions on Graphics (TOG)*, 42(4):1–18, 2023. 1, 4
- [5] Alexei Baevski, Henry Zhou, Abdelrahman Mohamed, and Michael Auli. wav2vec 2.0: A framework for self-supervised learning of speech representations. *arXiv: Computation and Language, arXiv: Computation and Language*, 2020. 4
- [6] Junming Chen, Yunfei Liu, Jianan Wang, Ailing Zeng, Yu Li, and Qifeng Chen. Diffsheg: A diffusion-based approach for real-time speech-driven holistic 3d expression and gesture generation. In *Proceedings of the IEEE/CVF Conference on Computer Vision and Pattern Recognition*, pages 7352–7361, 2024. 1
- [7] Kiran Chhatre, Radek Dan??ek, Nikos Athanasiou, Giorgio Becherini, Christopher Peters, Michael J. Black, and Timo Bolkart. Emotional speech-driven 3d body animation via disentangled latent diffusion. In *Proceedings of the IEEE/CVF Conference on Computer Vision and Pattern Recognition (CVPR)*, pages 1942–1953, 2024. 1
- [8] Jacob Devlin, Ming-Wei Chang, Kenton Lee, and Kristina Toutanova. BERT: Pre-training of deep bidirectional transformers for language understanding. In *Proceedings of the 2019 Conference of the North American Chapter of the Association for Computational Linguistics: Human Language Technologies, Volume 1 (Long and Short Papers)*, pages 4171–4186, Minneapolis, Minnesota, 2019. Association for Computational Linguistics. 5
- [9] Ylva Ferstl, Michael Neff, and Rachel McDonnell. Multi-objective adversarial gesture generation. *Proceedings of the 12th ACM SIGGRAPH Conference on Motion, Interaction and Games*, 2019. 3
- [10] Ylva Ferstl, Michael Neff, and Rachel McDonnell. Adversarial gesture generation with realistic gesture phasing. *Comput. Graph.*, 89:117–130, 2020. 3
- [11] Yarin Gal and Zoubin Ghahramani. A theoretically grounded application of dropout in recurrent neural networks. In *Neural Information Processing Systems*, 2015. 3
- [12] Ian Goodfellow, Jean Pouget-Abadie, Mehdi Mirza, Bing Xu, David Warde-Farley, Sherjil Ozair, Aaron Courville, and Yoshua Bengio. Generative adversarial networks. *Communications of the ACM*, 63(11):139–144, 2020. 1
- [13] Chuan Guo, Yuxuan Mu, Muhammad Gohar Javed, Sen Wang, and Li Cheng. Momask: Generative masked modeling of 3d human motions. In *Proceedings of the IEEE/CVF Conference on Computer Vision and Pattern Recognition*, pages 1900–1910, 2024. 1, 2
- [14] Ikhsanul Habibie, Weipeng Xu, Dushyant Mehta, Lingjie Liu, Hans-Peter Seidel, Gerard Pons-Moll, Mohamed Elgharib, and Christian Theobalt. Learning speech-driven 3d conversational gestures from video. In *Proceedings of the 21st ACM International Conference on Intelligent Virtual Agents*, pages 101–108, 2021. 2, 3, 6
- [15] Dai Hasegawa, Naoshi KANEKO, Shinichi Shirakawa, Hiroshi Sakuta, and Kazuhiko Sumi. Evaluation of speech-to-gesture generation using bi-directional lstm network. 2018. 3
- [16] Jonathan Ho and Tim Salimans. Classifier-free diffusion guidance. *arXiv preprint arXiv:2207.12598*, 2022. 3, 5, 6
- [17] Jonathan Ho, Ajay Jain, and Pieter Abbeel. Denoising diffusion probabilistic models. *Advances in neural information processing systems*, 33:6840–6851, 2020. 1
- [18] Diederik P Kingma. Auto-encoding variational bayes. *arXiv preprint arXiv:1312.6114*, 2013. 1
- [19] Michael Kipp. Gesture generation by imitation: from human behavior to computer character animation. 2005. 3
- [20] Alexander Kolesnikov, Alexey Dosovitskiy, Dirk Weissenborn, Georg Heigold, Jakob Uszkoreit, Lucas Beyer, Matthias Minderer, Mostafa Dehghani, Neil Houlsby, Sylvain Gelly, Thomas Unterthiner, and Xiaohua Zhai. An image is worth 16x16 words: Transformers for image recognition at scale. 2021. 2, 5
- [21] Stefan Kopp, Brigitte Krenn, Stacy Marsella, Andrew N. Marshall, Catherine Pelachaud, Hannes Pirker, Kristinn R. Thórisson, and Hannes Högni Vilhjálmsson. Towards a common framework for multimodal generation: The behavior markup language. In *International Conference on Intelligent Virtual Agents*, 2006. 3
- [22] Taras Kucherenko, Dai Hasegawa, Gustav Henter, Naoshi Kaneko, and Hedvig Kjellström. Analyzing input and output representations for speech-driven gesture generation. pages 97–104, 2019. 3
- [23] Taras Kucherenko, Pieter Wolfert, Youngwoo Yoon, Carla Viegas, Teodor Nikolov, Mihail Tsakov, and Gustav Eje Henter. Evaluating gesture generation in a large-scale open challenge: The genea challenge 2022. *ACM Transactions on Graphics*, 43:1 – 28, 2023. 7
- [24] Doyup Lee, Chiheon Kim, Saehoon Kim, Minsu Cho, and Wook-Shin Han. Autoregressive image generation using residual quantization. In *Proceedings of the IEEE/CVF Conference on Computer Vision and Pattern Recognition (CVPR)*, pages 11523–11532, 2022. 1, 6
- [25] Jing Li, Di Kang, Wenjie Pei, Xuefei Zhe, Ying Zhang, Zhenyu He, and Linchao Bao. Audio2gestures: Generating diverse gestures from speech audio with conditional variational autoencoders. In *2021 IEEE/CVF International Conference on Computer Vision (ICCV)*, pages 11273–11282, 2021. 4
- [26] Tianye Li, Timo Bolkart, Michael J Black, Hao Li, and Javier Romero. Learning a model of facial shape and expression from 4d scans. *ACM Trans. Graph.*, 36(6):194–1, 2017. 4, 6
- [27] Han Liang, Jiacheng Bao, Ruichi Zhang, Sihan Ren, Yuecheng Xu, Sibe Yang, Xin Chen, Jingyi Yu, and Lan Xu. Omg: Towards open-vocabulary motion generation via mixture of controllers. In *Proceedings of the IEEE/CVF Conference on Computer Vision and Pattern Recognition*, pages 482–493, 2024. 1

- [28] Haiyang Liu, Zihao Zhu, Naoya Iwamoto, Yichen Peng, Zhengqing Li, You Zhou, Elif Bozkurt, and Bo Zheng. Beat: A large-scale semantic and emotional multi-modal dataset for conversational gestures synthesis. In *European conference on computer vision*, pages 612–630. Springer, 2022. 1
- [29] Haiyang Liu, Zihao Zhu, Giorgio Becherini, Yichen Peng, Mingyang Su, You Zhou, Xuefei Zhe, Naoya Iwamoto, Bo Zheng, and Michael J Black. Emage: Towards unified holistic co-speech gesture generation via expressive masked audio gesture modeling. In *Proceedings of the IEEE/CVF Conference on Computer Vision and Pattern Recognition*, pages 1144–1154, 2024. 1, 4, 6
- [30] Xian Liu, Qianyi Wu, Hang Zhou, Yinghao Xu, Rui Qian, Xinyi Lin, Xiaowei Zhou, Wayne Wu, Bo Dai, and Bolei Zhou. Learning hierarchical cross-modal association for co-speech gesture generation. In *Proceedings of the IEEE/CVF Conference on Computer Vision and Pattern Recognition*, pages 10462–10472, 2022. 7
- [31] Yifei Liu, Qiong Cao, Yandong Wen, Huaiguang Jiang, and Changxing Ding. Towards variable and coordinated holistic co-speech motion generation. In *Proceedings of the IEEE/CVF Conference on Computer Vision and Pattern Recognition*, pages 1566–1576, 2024. 1, 2, 6
- [32] William Peebles and Saining Xie. Scalable diffusion models with transformers. In *Proceedings of the IEEE/CVF International Conference on Computer Vision (ICCV)*, pages 4195–4205, 2023. 1
- [33] Xingqun Qi, Hengyuan Zhang, Yatian Wang, Jiahao Pan, Chen Liu, Peng Li, Xiaowei Chi, Mengfei Li, Qixun Zhang, Wei Xue, et al. Cocogesture: Toward coherent co-speech 3d gesture generation in the wild. *arXiv preprint arXiv:2405.16874*, 2024. 1
- [34] Robin Rombach, Andreas Blattmann, Dominik Lorenz, Patrick Esser, and Björn Ommer. High-resolution image synthesis with latent diffusion models. *CoRR*, abs/2112.10752, 2021. 1
- [35] Xu Shi, Chuanchen Luo, Junran Peng, Hongwen Zhang, and Yunlian Sun. Fg-mdm: Towards zero-shot human motion generation via chatgpt-refined descriptions. 2023. 1
- [36] Jiaming Song, Chenlin Meng, and Stefano Ermon. Denoising diffusion implicit models. In *International Conference on Learning Representations*, 2021. 1
- [37] Nitish Srivastava, Geoffrey Hinton, Alex Krizhevsky, Ilya Sutskever, and Ruslan Salakhutdinov. Dropout: a simple way to prevent neural networks from overfitting. *The journal of machine learning research*, 15(1):1929–1958, 2014. 3
- [38] Shanlin Sun, Gabriel De Araujo, Jiaqi Xu, Shenghan Zhou, Hanwen Zhang, Ziheng Huang, Chenyu You, and Xiaohui Xie. Coma: Compositional human motion generation with multi-modal agents, 2025. 6
- [39] Sarah L. Taylor, John T. Windle, David Greenwood, and Iain Matthews. Speech-driven conversational agents using conditional flow-vaes. *Proceedings of the 18th ACM SIGGRAPH European Conference on Visual Media Production*, 2021. 4
- [40] Guy Tevet, Brian Gordon, Amir Hertz, Amit H Bermano, and Daniel Cohen-Or. Motionclip: Exposing human motion generation to clip space. In *European Conference on Computer Vision*, pages 358–374. Springer, 2022. 1
- [41] Yating Tian, Hongwen Zhang, Yebin Liu, and Limin Wang. Recovering 3d human mesh from monocular images: A survey. *IEEE Transactions on Pattern Analysis and Machine Intelligence*, 45(12):15406–15425, 2023. 1
- [42] Aaron Van Den Oord, Oriol Vinyals, et al. Neural discrete representation learning. *Advances in neural information processing systems*, 30, 2017. 1, 4, 6
- [43] Ashish Vaswani, Noam Shazeer, Niki Parmar, Jakob Uszkoreit, Llion Jones, Aidan N Gomez, Łukasz Kaiser, and Illia Polosukhin. Attention is all you need. In *Advances in Neural Information Processing Systems*. Curran Associates, Inc., 2017. 6
- [44] Petra Wagner, Zofia Malisz, and Stefan Kopp. Gesture and speech in interaction: An overview. *Speech Commun.*, 57: 209–232, 2014. 3
- [45] Wei Yao, Hongwen Zhang, Yunlian Sun, and Jinhui Tang. Staf: 3d human mesh recovery from video with spatio-temporal alignment fusion. *IEEE Transactions on Circuits and Systems for Video Technology*, pages 1–1, 2024. 1
- [46] Hongwei Yi, Hualin Liang, Yifei Liu, Qiong Cao, Yandong Wen, Timo Bolkart, Dacheng Tao, and Michael J Black. Generating holistic 3d human motion from speech. In *Proceedings of the IEEE/CVF Conference on Computer Vision and Pattern Recognition*, pages 469–480, 2023. 1, 2, 4, 6, 8
- [47] Youngwoo Yoon, Bok Cha, Joo-Haeng Lee, Minsu Jang, Jaeyeon Lee, Jaehong Kim, and Geehyuk Lee. Speech gesture generation from the trimodal context of text, audio, and speaker identity. *ACM Transactions on Graphics (TOG)*, 39(6):1–16, 2020. 7
- [48] Hongwen Zhang, Yating Tian, Xinchu Zhou, Wanli Ouyang, Yebin Liu, Limin Wang, and Zhenan Sun. Pymaf: 3d human pose and shape regression with pyramidal mesh alignment feedback loop. In *Proceedings of the IEEE/CVF International Conference on Computer Vision (ICCV)*, pages 11446–11456, 2021. 1
- [49] Hongwen Zhang, Yating Tian, Yuxiang Zhang, Mengcheng Li, Liang An, Zhenan Sun, and Yebin Liu. Pymaf-x: Towards well-aligned full-body model regression from monocular images. *IEEE Transactions on Pattern Analysis and Machine Intelligence*, 45(10):12287–12303, 2023. 1
- [50] Jianrong Zhang, Yangsong Zhang, Xiaodong Cun, Yong Zhang, Hongwei Zhao, Hongtao Lu, Xi Shen, and Ying Shan. Generating human motion from textual descriptions with discrete representations. In *Proceedings of the IEEE/CVF conference on computer vision and pattern recognition*, pages 14730–14740, 2023. 1
- [51] Zeyi Zhang, Tenglong Ao, Yuyao Zhang, Qingzhe Gao, Chuan Lin, Baoquan Chen, and Libin Liu. Semantic gesticulator: Semantics-aware co-speech gesture synthesis. *ArXiv*, abs/2405.09814, 2024. 1
- [52] Yang Zhou, Jimei Yang, Dingzeyu Li, Jun Saito, Deepali Aneja, and Evangelos Kalogerakis. Audio-driven neural gesture reenactment with video motion graphs. *2022 IEEE/CVF Conference on Computer Vision and Pattern Recognition (CVPR)*, pages 3408–3418, 2022. 4
- [53] Lingting Zhu, Xian Liu, Xuanyu Liu, Rui Qian, Ziwei Liu, and Lequan Yu. Taming diffusion models for audio-driven co-speech gesture generation. In *Proceedings of*

*the IEEE/CVF Conference on Computer Vision and Pattern Recognition (CVPR), pages 10544–10553, 2023.* [1](#)